Quality assurance of the multi-center trial Prostate Cancer localization with a Multiparametric MR Approach (PCaMAP): initial results

Marnix C. Maas[1], Jurgen J. Fütterer[1], and Tom W.J. Scheenen[1]

[1]Radiology, Radboud University Nijmegen Medical Centre, Nijmegen, GLD, Netherlands

Introduction

In the prospective multi-centre PCaMAP study (Clinicaltrials.gov identifier NCT01138527) the primary objective is to prove the diagnostic accuracy of 3T multi-modality MR imaging in distinguishing carcinoma from other prostate tissue, with whole-mount section histopathology of resected prostates as the gold standard. The performance of measurements obtained on clinical MRI systems in this trial is monitored with phantom measurements, dedicated to the different MR techniques implemented in the protocol. Next to high resolution T2-weighted anatomical imaging the protocol comprises three functional MR techniques: quantitative diffusion weighted imaging (DWI), dynamic contrast enhanced (DCE) imaging and 1H-spectroscopic imaging (MRSI). Quantitative results of the PCaMAP protocol of three dedicated phantoms all measured across different MR systems under standardised conditions can identify system-related variations in functional parameters. Here we present preliminary results of this study, in which data from 5 institutions are included.

Methods

Scans were performed by the same operator using the same three phantoms on all sites on Siemens 3T MRI systems (Trio with Tim [4 sites] or Verio [1 site], Siemens Healthcare, Erlangen) using the external body array and spine array as receive coils. All measurements were performed according to the protocol used in the patient study. The diffusion phantom consisted of a 8L cylindrical container containing ice water and 5 sealed inner tubes filled with distilled water and one tube with sucrose (Fig 1a). Diffusion weighted imaging (DWI) was performed with a spin-echo EPI sequence (TR/TE 3300/60 ms, resolution 2.2x1.6x3.6 mm, b-values 0, 100, 400, 800 s/mm^2, scan time 4.6 min). ADC maps were calculated by fitting monoexponential decay curves to each voxel. Circular ROIs were drawn in regions within each tube in a central image slice. T_1 calibration was performed with a doped-water-filled phantom with inserts for 12 test tubes filled with gels with various concentrations of Gd, [Eurospin II Magnetic Resonance Quality Assessment Test Object No. 5 (figure 1b)]. T_1 relaxation times were measured in a progressive saturation experiment with fixed TR and varying flip angle, using a spoiled gradient echo (SPGR) sequence with flip angles (FA) of 2°, 5°, 10° and 20° (TR/TE 3.9/1.4 ms, resolution 1.63x1.63x3.6 mm, 4 averages, scan time 37 s per FA). The signal curve in each voxel was linearized, and T_1 maps were created by linear least-squares fits to the transformed data [1]. T_1 values reported represent means of circular ROIs placed within a tube on a single slice. The spectroscopy phantom consisted of a glass sphere containing a solution of relevant metabolites for the prostate (citrate, choline, creatine and spermine in concentrations of 90, 10, 12 and 18 mmol/L respectively) within a container with sunflower oil. 3D MRSI was performed with a PRESS sequence (TR/TE 750/145 ms, voxel size 8.0x8.0x8.0 mm, 6 averages, acquisition time 8.2 min). Spectra were processed using Metabolite Report (Siemens Healthcare, Erlangen, Germany), which automatically phased and fitted the spectra accounting for contributions of choline (Cho), creatine (Cr), citrate (Ci) and spermine (Sp). Between 9 and 15 voxels were selected in each scan based on spectral quality (shim and SNR) and goodness of fit, and the ratio of (Cho + Sp + Cr)/Ci [CSCC] was calculated.

Results and discussion

The mean ADC across all sites and across the 5 water tubes within a central slice was $1127 \cdot 10^{-6}$ mm^2/s (Fig. 2). Comparing tubes at similar positions in the FOV across institutions yielded differences between $65 \cdot 10^{-6}$ mm^2/s (6% of average) and $108 \cdot 10^{-6}$ mm^2/s (10% of average) for water tubes and $116 \cdot 10^{-6}$ mm^2/s (21% of average) for sucrose. The maximum ADC difference between any two water tubes within the same slice was $82 \cdot 10^{-6}$ mm^2/s. Marginally significant systematic differences across institutions were found using Friedman's non-parametric two-way Anova test for repeated measures (p=0.04). T_1 relaxation times observed in all tubes in a central slice were similar across sites (Fig. 3). The SD across sites of ROI-averaged T_1 values for a single tube relative to the overall mean for this tube was 7% averaged over all tubes; the maximum observed relative difference across sites for a single tube was 22%. Significant differences in observed T_1 values between sites were found (Friedman's test for repeated measures, p<0.0005). These differences could be caused by differences in flip angle calibrations, which could occur across sites, but could also occur within one experiment due to B_1^+ inhomogeneities. T_1 profiles along the scanner axis of the same test tube for all sites showed differences between the central slices and slices closer to the edge of the phantom (Fig. 3), indeed likely due to flip angle inhomogeneity. Mean CSCC ratios as measured by 3D MRSI differed by no more than 0.11 (21% of the overall mean of 0.51, Fig. 4), and differences between sites were found to be significant (Kruskal-Wallis test, p<0.0001).

Conclusions

Quality control measurements for multi-modality MR at 3T using a standardized protocol and MR systems of the same vendor at multiple institutions yielded relatively homogeneous results. Marginally significant differences in measured ADC values were observed between institutions, but variations within a single examination tended to be larger. Significant differences in T_1 values between sites were observed. CSCC ratios measured by MRSI differed by only 21% across sites, and these differences were also significant. Whether these results warrant correction of data collected in the patient study should be assessed by comparing the observed variations with those found in repeated measurements and by including data from the remaining institutions participating in the patient study.

References:

[1]   Cheng, *MRM* 55:566-574 (2006)

Figure 2. *ADCs at different locations in the FOV. C: central axis; LA: left anterior; RA: right anterior; LP: left posterior; RP: right posterior*

Figure 3. *T1 relaxation times in all tubes in a central slice.*

Figure 4. *Results of the spectroscopy measurements. Horizontal lines represent means of observed values.*
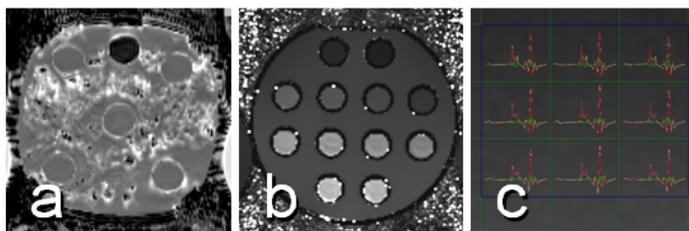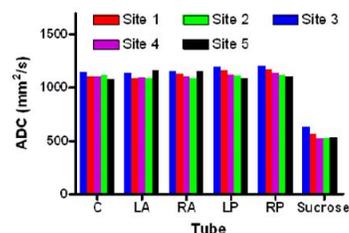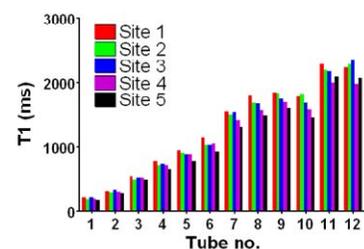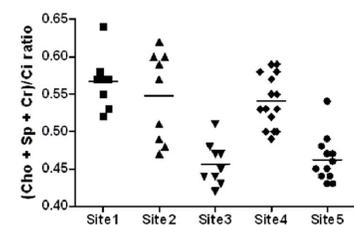

Figure 1. *ADC map of the diffusion phantom (a), T_1 map of the T_1 phantom and spectral overlay map (c) showing measured spectra (white) with fits (red) and residuals (green).*